Data Repository item 2008091

Evidence for Mechanically Coupled Lithosphere in Central Asia and Resulting Implications – Supplementary Materials

Chun-Yong Wang, Lucy M. Flesch, Paul G. Silver, Li-Jun Chang, Winston W. Chan

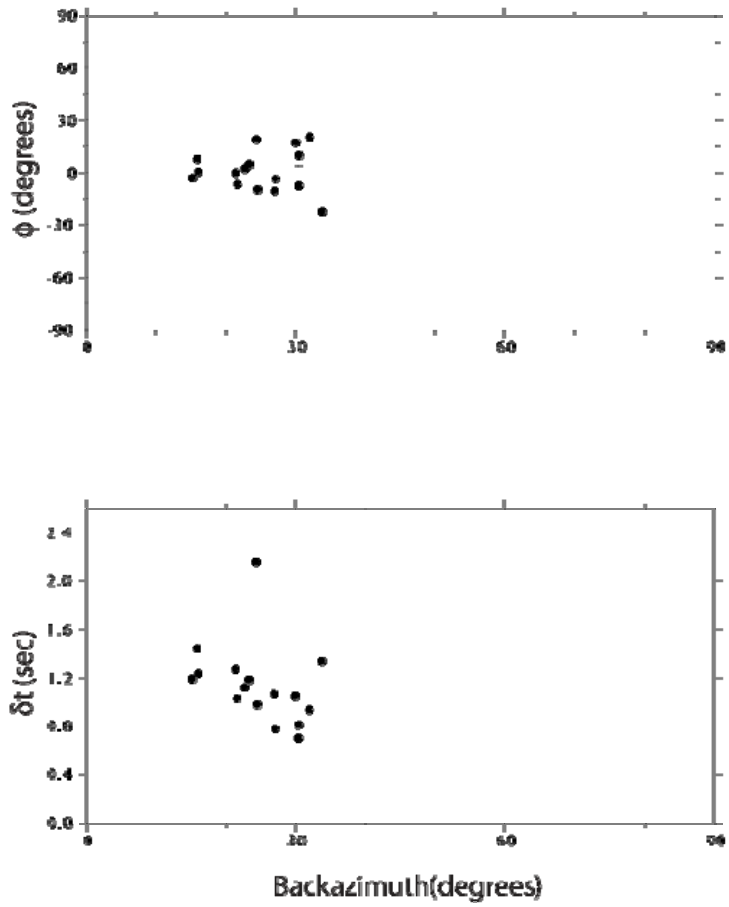

Figure DR1. Individual estimates of splitting parameters ϕ and δt as a function of backazimuth modulo 90º for permanent station LUQ (see Table S1 for location). If two or more anisotropic layers are present in the medium, both parameters should show systemic variation as a function of back azimuth on such a plot (Silver and Savage, 1994). While there is significant scatter in

the individual observations, there is no clear sign of the systematic variation normally observed when two layers are present.

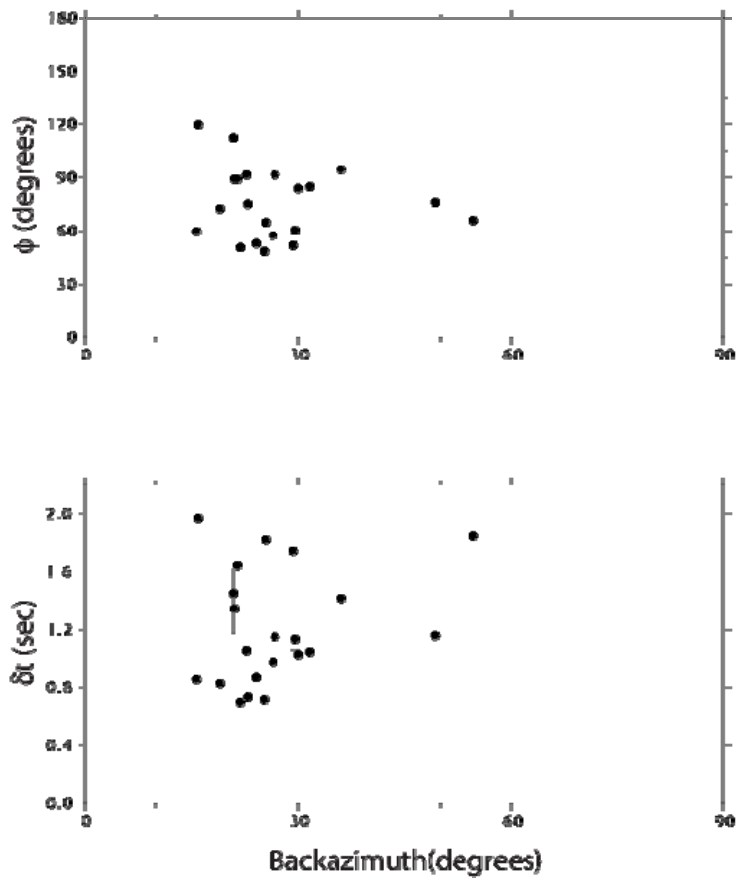

Figure DR2. Same as **DR1 for** Station YLO.

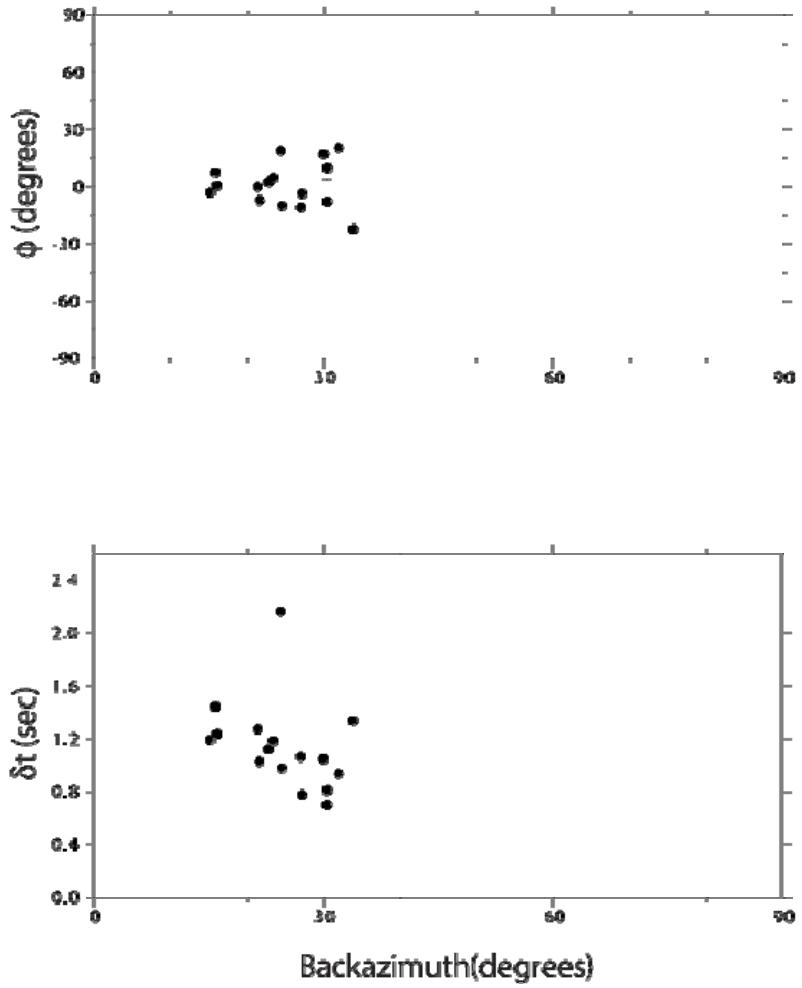

Figure DR3. Same as **DR1 for** station YSH.

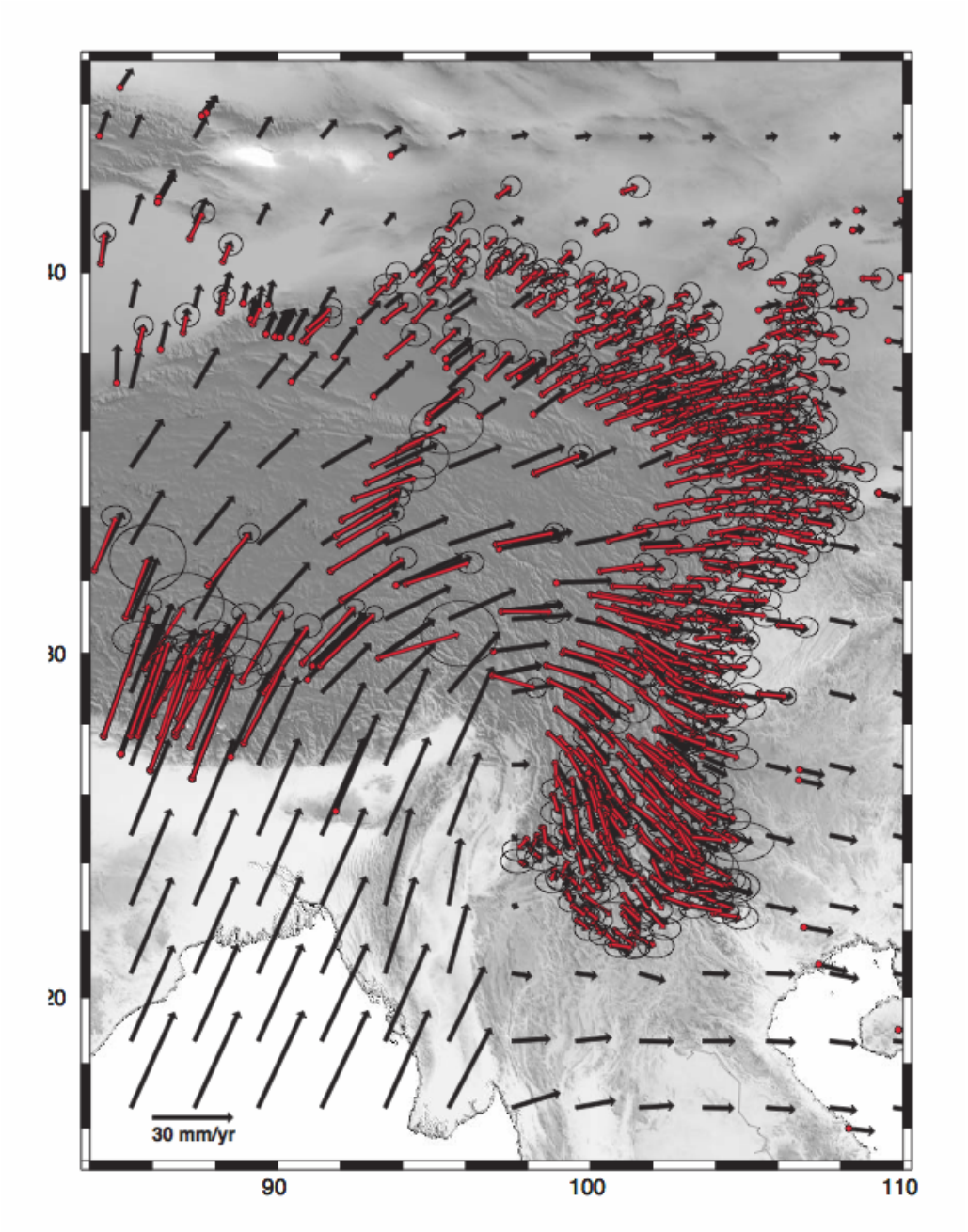

Figure DR4a. The surface velocity field determined from GPS observations and Quaternary fault slip data, used in this study. The model velocity field (black arrows) and GPS observations (red arrows) from Zhang et al. (2004) plotted in a Eurasian-fixed reference frame. Additional GPS data used is represented by red dots for clarity. Plot is shown in degrees east and north.

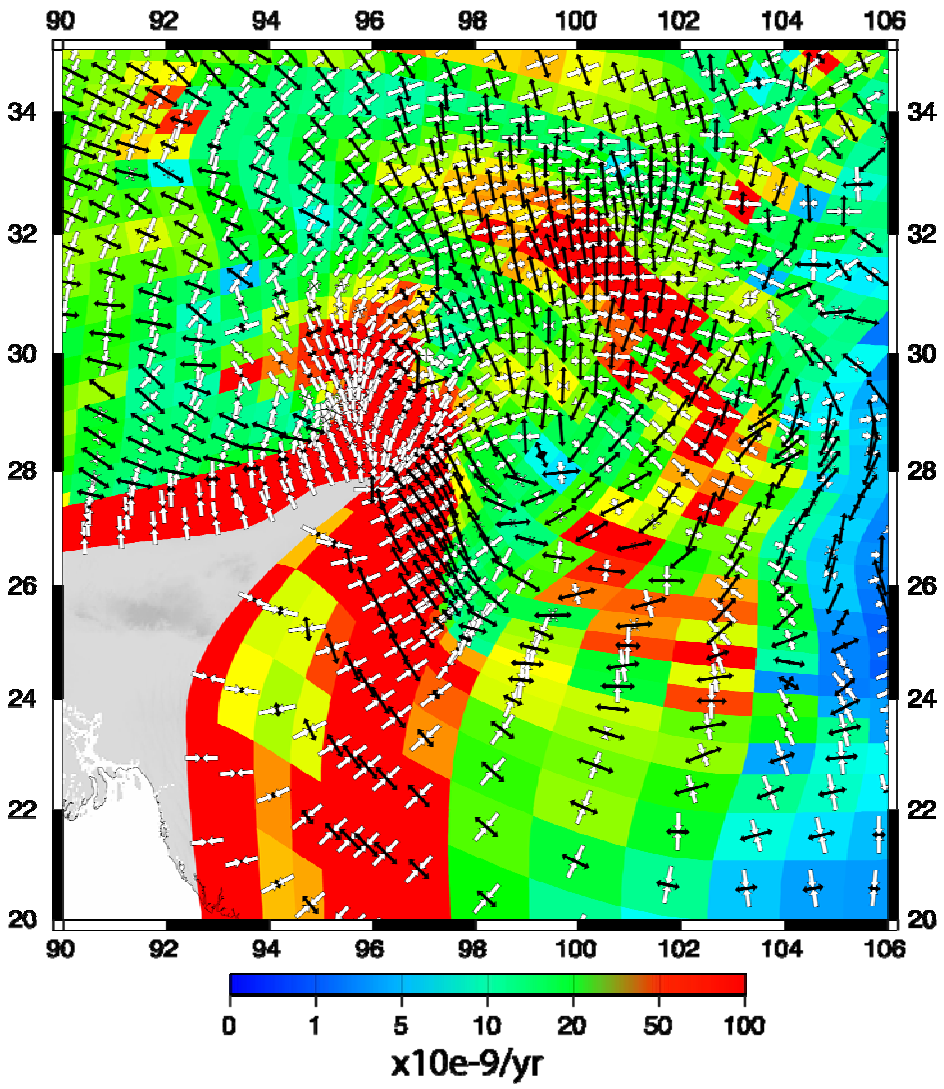

Figure DR4b. The surface deformation field represented as continuous strain rates associated with the velocities in Figure S4a. Extensional strains are represented as black arrows, compressional strains with white arrows. Strain tensors have been normalized and strain magnitudes are represented as the grid background. Note that at about latitude 28º, longitude 100º, there is a north-to-south transition from NS extension to EW extension. Plot is shown in degrees east and north.

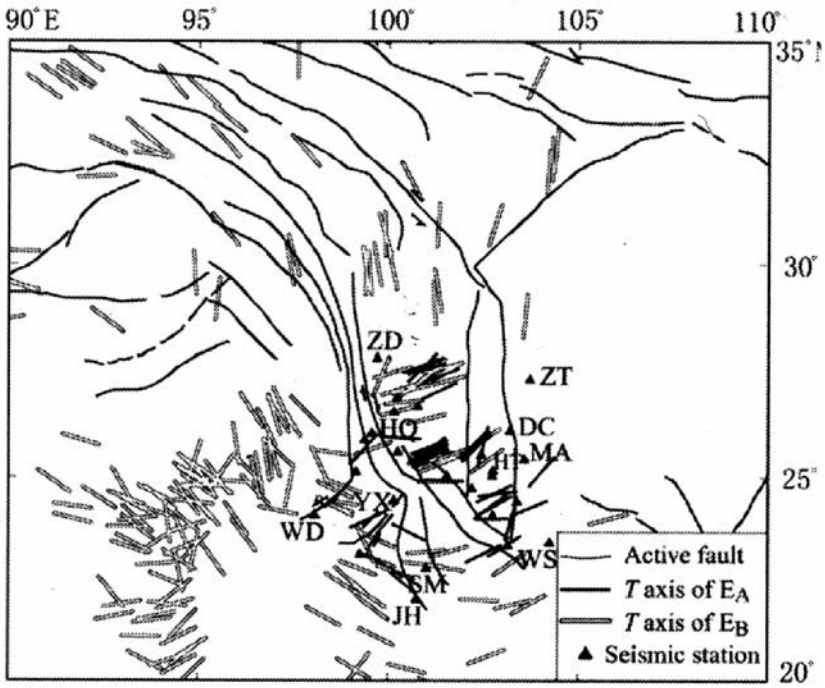

Figure DR5. T-axes of regional seismicity from the CMT catalog (open bars) and catalog of small regional events (filled bars) (Wu et al., 2004). For pure shear, these axes should be parallel to instantaneous direction of maximum extension. These directions follow closely the maximum extension direction determined from GPS and Quaternary fault data (Figure S4b) and values of ϕ (Figure 2), all of which show the abrupt change in orientation at a latitude around 27º-29º.

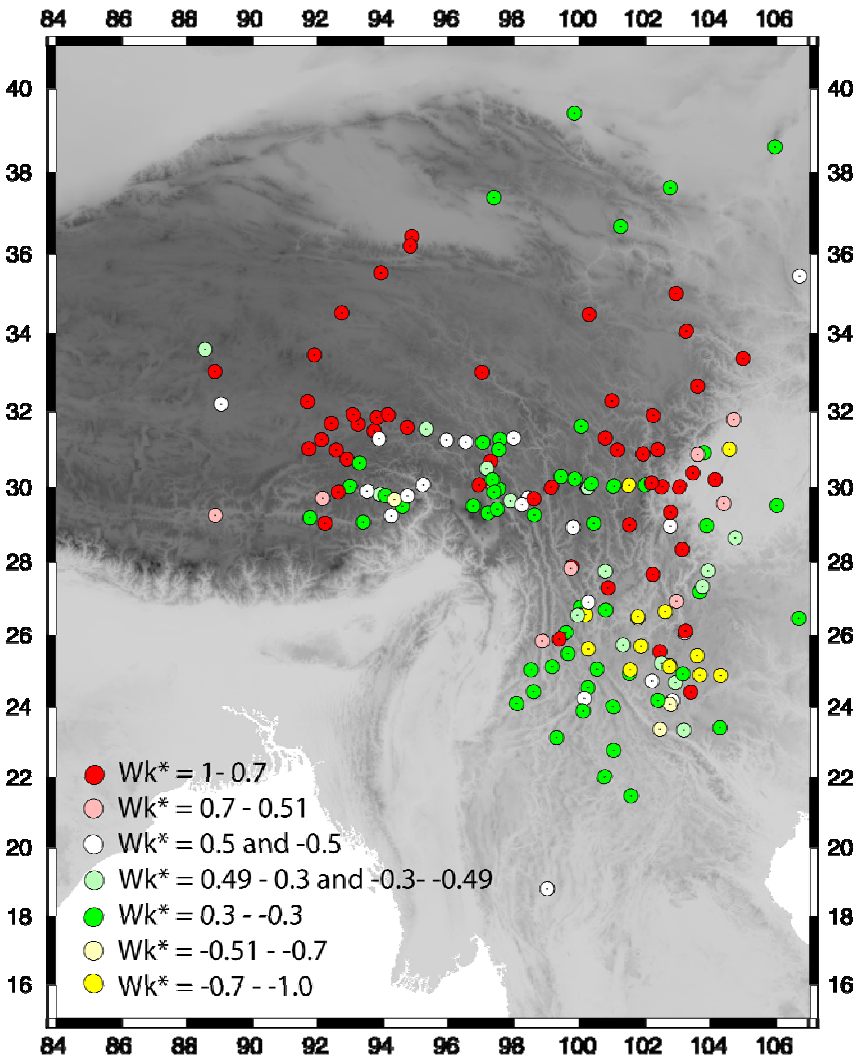

Figure DR6. The kinematic vorticity number, W^*_k (see legend) calculated at each splitting station. Plot is shown in degrees east and north.

Kinematic Vorticity Number

We calculate the kinematic vorticity number W_k (McKenzie, 1979; Means, 1990; Fossen and Tikoff, 1993) that is used to distinguish which of the three surface predictions, ϕ_{ssl}, ϕ_{ssr} and ϕ_{ps}, should be compared with the mantle anisotropy. In two dimensions, the kinematic vorticity number is defined as $W_k = \frac{\sqrt{2}\dot{\omega}}{\sqrt{2\dot{\varepsilon}_{xx}^2 + 2\dot{\varepsilon}_{yy}^2 + 2\dot{\varepsilon}_{xy}^2}}$ (equation 4 from Tikoff and Fossen (1995)), where $\dot{\varepsilon}_{xx}$, $\dot{\varepsilon}_{yy}$, and $\dot{\varepsilon}_{xy}$ are the components of $\dot{\varepsilon}_c$, and $\dot{\omega}$ is the rotational component of $\mathbf{L}_c$. Therefore,

W_k = ±1 for left/right lateral simple shear and 0 for pure shear, in the absence of rigid-body rotation (Kaminski and Ribe, 2002). If there is external rigid-body rotation unrelated to the internal deformation generating the anisotropy, however, W_k will not predict the correct style of deformation. We therefore estimate the amount of external rotation in $\mathbf{L}_c$, $\frac{\partial\theta}{\partial t}$, using the line rotation method (Lamb, 1987; Holt and Haines, 1993) $\frac{\partial\theta}{\partial t} = \dot{\omega} + \dot{\varepsilon}_{xy}\cos 2\theta + \frac{1}{2}\left[\dot{\varepsilon}_{yy} - \dot{\varepsilon}_{xx}\right]\sin 2\theta$ (equation A10 from Holt and Haines, 1993), assuming that the observed splitting orientation constitutes a deformational invariant direction, θ. The external rotation is then subtracted from $\dot{\omega}$ to determine a $\dot{\omega}^*$ associated only with internal deformation that is then used to calculate a corrected value for W_k, denoted as W^*_k. This corrected W^*_k is then used to choose ϕ_c. An independent check of this procedure is that a map of the remaining external rotation, $\frac{\partial\theta}{\partial t}$, should produce zones experiencing rigid-body rotation (no internal deformation), bounded by major faults. Indeed the resulting rotational field has this property.

Outliers

Of the 178 observations there is a small subset, 14 points or about 8% of the data set, that have very large misfits, over 70º. We do not presently know the reason for these large values, although there are several possibilities that we are presently pursuing. First, in many of these cases, there is a large areal-strain component, which, for an incompressible medium corresponds to a non-zero vertical strain. However, our equation for W_k assumes that the deformation is strictly horizontal. This can bias W_k to low values, and hence to the wrong axis. Second, several of these points are located along the eastern edge of our study area, in the vicinity of the stable Sechuan basin. There is reduced present-day deformation here, so that there is an added

possibility that the splitting is sensitive to fossil anisotropy, in addition to present-day mantle deformation. Finally, there may be uncertainties in these particular splitting measurements that are not well reflected in the formal uncertainties.

Table DR1. Splitting parameters for SKS phases in study area

Station code	Location		ϕ (º)	±(º)	δt (s)	± (s)	Number of Events	Quality	Remark
	Lat. (º)	Long. (º)							
BAS	30.06	96.91	81.7	10.0	0.58	0.05	4	A	6
BAT	30.00	99.12	145.4	3.4	0.62	0.10	8	A	3
BDA	30.20	97.31	131.0	1.8	1.21	0.14	7	A	6
BMI	29.81	95.82	000	00	000	00	16	*	6
BSH	25.12	99.15	114.0	4.7	0.69	0.31	4	A	2
CAD	31.00	97.50	147.4	2.5	0.90	0.07	20	A	1
CAY	23.13	99.26	120.8	1.9	1.23	0.20	7	A	2
CD2	30.91	103.76	124.9	2.4	1.00	0.12	12	A	1
CHJ	24.68	102.92	81.6	7.7	0.78	0.05	1	A	7
CUX	25.03	101.54	111.1	2.2	1.06	0.20	11	A	2
DAB	30.88	101.90	142.1	3.9	1.03	0.15	4	A	6
DBU	34.06	103.23	100.9	6.8	1.03	0.18	5	A	4
DFU	30.99	101.12	140.3	6.6	0.81	0.15	3	A	6
DGN	27.76	103.89	142.8	6.6	0.59	0.12	4	A	7
DLH	37.38	97.38	105.2	3.1	0.70	0.08	7	A	5
DNB	29.54	98.24	139.7	14.6	0.53	0.21	9	A	6
DUC	26.11	103.20	8.9	5.0	0.62	0.14	4	A	2
EMS	29.58	103.45	000	0	000	00	3	C	3, S
ESH	24.18	102.39	92.5	5.0	1.05	0.30	2	B	7
EYA	26.06	99.56	103.7	3.3	1.03	0.11	13	A	2
FUM	25.22	102.49	131.5	3.3	1.32	0.26	4	B	7
GAZ	31.61	100.02	167.6	9.3	1.28	0.39	2	B	6
GDS	30.06	101.97	12.2	3.7	0.60	0.13	7	A	3

GEJ	23.35	103.15	88.8	4.0	0.99	0.07	13	A	2
GOM	36.43	94.87	88.4	2.8	1.02	0.09	28	A	1
GTA	39.41	99.81	127.2	3.5	0.76	0.14	13	A	1
GUN	30.12	102.17	165.7	11.4	0.79	0.25	6	A	6
GYA	26.46	106.66	160.5	6.8	0.52	0.04	18	A	1
HDN	26.64	102.58	83.7	6.5	0.56	0.11	6	A	7
HEQ	26.55	100.15	132.1	3.3	0.76	0.10	23	A	2
HEZ	35.01	102.91	119.9	2.5	1.33	0.16	5	A	4
HHE	23.37	102.42	104.0	6.0	1.41	0.34	2	B	7
HLI	26.65	102.25	000	00	000	00	2	C	7
HLS	29.26	98.61	172.7	14.4	0.87	0.16	2	B	6
HLT	25.15	102.75	86.7	3.9	0.75	0.21	6	A	2
HMS	29.57	104.39	138.2	1.5	0.73	0.09	5	A	3, S
HNI	30.22	99.82	175.5	3.6	1.24	0.08	10	A	6
HOL	30.10	100.33	0.8	6.1	1.08	0.22	3	B	6
HWS	28.64	104.74	133.8	5.6	0.58	0.05	6	A	3, S
HYQ	36.67	101.25	117.6	3.8	1.17	0.20	6	A	5
JHO	22.02	100.74	115.4	1.3	0.83	0.11	5	A	2
JJS	31.01	104.54	108.7	2.6	0.67	0.13	7	A	3
KMI	25.12	102.74	94.0	8.1	0.56	0.10	12	A	1
LGH	27.41	100.86	000	00	000	00	4	Null	3, S
LIJ	26.90	100.23	8.2	2.6	1.71	0.13	16	A	2
LIT	30.00	100.24	111.9	3.8	1.13	0.32	6	A	6
LNZ	29.67	94.34	100.5	3.6	0.90	0.17	3	B	6
LUH	31.30	100.75	129.1	7.7	1.15	0.27	6	A	6
LUL	29.77	94.74	92.6	4.9	0.52	0.12	2	B	6
LUP	24.88	104.30	93.1	4.5	1.37	0.17	1	B	7
LUQ	25.54	102.45	12.3	5.2	0.81	0.22	17	A	2
LZZ	29.52	106.01	123.8	1.1	1.61	0.25	4	A	3
MAL	25.43	103.58	106.0	5.9	0.89	0.28	8	A	2
MAQI	34.48	100.25	131.8	3.0	0.82	0.10	4	A	5
MDS	30.07	103.04	000	00	000	00	3	C	3, S

MEK	31.89	102.22	142.5	7.1	0.54	0.07	7	A	3
MIL	24.41	103.39	43.1	1.5	1.21	0.11	13	A	2
MNK	29.70	98.60	137.2	5.6	0.86	0.21	8	A	6
PIL	35.45	106.68	129.9	2.9	0.83	0.10	8	A	4
PZH	26.50	101.74	108.7	4.9	1.18	0.21	15	A	1
QJA	26.92	102.92	1.5	5.1	0.88	0.10	1	A	7
RTA	32.27	100.98	147.2	3.7	1.31	0.07	7	A	3
SHG	37.62	102.76	127.9	1.5	1.08	0.11	6	A	4
SHR	29.53	96.41	000	00	000	00	7	*	6
SOA	32.65	103.60	135.5	3.8	1.46	0.27	3	B	3
SOM	25.35	103.03	000	00	000	00	3	C	7
SMO	22.78	101.01	94.5	0.9	1.04	0.08	8	A	2
TCG	25.03	98.52	119.8	5.1	1.47	0.26	7	A	1
THI	24.07	102.75	104.0	1.9	1.19	0.08	11	A	2
TMY	30.06	95.20	107.8	3.6	0.99	0.18	3	A	6
TSH	25.61	100.25	113.5	2.4	1.28	0.11	4	A	2
TTO	29.88	97.38	139.3	7.2	0.67	0.10	6	A	6
WDA	29.42	97.48	133.6	8.4	0.72	0.10	9	A	6
WDI	24.09	98.07	118.0	1.9	0.88	0.16	9	A	2
WEC	31.48	103.59	000	00	000	00	4	C	6
WMP	29.05	103.79	000	00	000	00	5	C	3, S
WSH	23.41	104.25	80.0	5.5	1.40	0.08	9	A	2
WUD	33.36	104.99	104.0	8.0	1.30	0.20	4	A	4
XAC	28.93	99.80	172.4	4.9	0.83	0.05	3	A	3, S
XJP	29.34	102.77	168.5	4.5	0.50	0.01	12	A	3, S
YAJ	30.03	101.02	93.8	5.0	1.34	0.12	18	A	6
YAN	30.01	103.02	144.3	5.9	0.96	0.25	2	B	6
YCH	38.61	105.93	139.1	1.5	1.33	0.05	21	A	1
YGD	30.20	104.10	128.0	5.3	1.23	0.10	3	A	6
YID	30.29	99.40	5.7	3.7	0.61	0.08	6	A	6
YIL	24.92	103.15	57.3	6.0	0.60	0.31	3	B	7
YLO	25.89	99.37	77.0	2.8	0.96	0.04	22	A	2

YME	24.72	102.20	99.6	6.2	0.93	0.10	9	A	2
YMO	25.69	101.86	110.0	6.1	0.71	0.28	2	B	7
YSH	26.69	100.77	175.4	5.5	0.72	0.10	16	A	2
YXI	24.24	100.14	111.5	1.3	0.97	0.06	8	A	2
YTS	32.49	105.72	00	000	00	000	10	*	3
YUS	33.01	97.02	111.3	2.9	1.33	0.24	3	A	5
YZP	30.87	103.57	144.9	7.9	0.82	0.31	3	B	6
ZHB	29.62	96.33	000	00	000	00	19	*	6
ZHD	27.82	99.70	178.0	4.9	0.82	0.20	7	A	2
ZJG	31.79	104.67	123.0	4.1	1.21	0.34	2	B	3, S
ZOT	27.32	103.72	134.2	1.9	1.08	0.11	12	A	2

Remarks:
ϕ is fast polarization, δt is delay time, and "±" denotes 2 standard deviations.
1, China National Seismograph Network (permanent)
2, Yunnan Regional Seismograph Network (permanent)
3, Sichuan Regional Seismograph Network (permanent)
4, Gansu Regional Seismograph Network (permanent)
5, Qinghai Regional Seismograph Network (permanent)
6, Sino-US Temporary Seismic Observation in western Sichuan and eastern Tibet in 2004-2006 (portable)
7, Temporary Seismic Observation in Yunnan in 2000-2001 (portable)
S, Short – period permanent station in Sichuan;
*, Scattering of the fast polarizations
Null. No splitting observed

Table DR2. The calculated kinematic vorticity W_k* for each splitting observation.

Long. (°)	Lat (°)	W_k*	Station
92.09	31.26	0.7	ES01
92.09	31.26	1.0	ES01
92.54	30.99	0.3	ES02
92.54	30.99	0.8	ES02
92.86	30.75	0.7	ES03
93.25	30.64	0.1	ES04
92.40	31.68	1.0	ES05
93.20	31.66	1.0	ES06
93.70	31.48	0.7	ES07
93.84	31.28	0.5	ES08
93.06	31.91	0.8	ES09
93.79	31.84	0.9	ES10
94.13	31.91	0.9	ES11
94.70	31.58	0.7	ES12
95.28	31.54	0.4	ES13
95.90	31.25	0.5	ES14
96.50	31.19	0.5	ES15
97.02	31.18	0.3	ES16

97.54	31.27	0.2	ES17
97.96	31.30	0.5	ES18
97.26	30.69	0.7	ES23
97.14	30.50	0.4	ES24
97.30	30.12	0.6	ES25
97.51	29.95	0.1	ES26
97.89	29.64	-0.4	ES27
98.42	29.72	0.5	ES28
97.19	29.32	0.1	ES30
96.75	29.51	-0.1	ES31
93.91	29.81	-0.4	ES36
93.51	29.90	-0.5	ES37
92.96	30.02	0.0	ES38
92.62	29.87	0.7	ES38
92.62	29.87	0.7	ES39
92.15	29.71	0.6	ES40
91.76	29.19	0.0	ES41
92.23	29.04	0.7	ES43
93.38	29.07	0.0	ES44
94.25	29.24	0.5	ES46
94.58	29.49	0.2	ES48
102.35	31.00	1.0	MC01
103.43	30.38	0.8	MC02
102.49	30.01	0.9	MC03
101.48	30.06	-1.0	MC04
100.22	29.99	0.3	MC05
99.79	28.94	0.9	MC06
100.42	29.04	-0.3	MC07
101.51	29.00	0.8	MC08
102.76	28.96	0.5	MC09
103.87	28.98	0.3	MC10
103.12	28.33	0.9	MC11
102.21	27.66	1.0	MC12
100.76	27.74	-0.4	MC13
99.74	27.86	0.7	MC14
99.99	26.76	-0.2	MC15
103.63	27.18	-0.2	MC16
101.74	26.47	-0.6	MC17
103.20	26.06	0.5	MC18
99.64	25.49	-0.1	MC21
100.24	24.53	-0.2	MC22
101.51	24.93	-0.1	MC23
102.83	24.17	-0.5	MC24
103.67	24.89	-0.8	MC25
102.74	25.12	-0.8	KMI
91.69	32.25	1.0	AMDO
96.91	30.06	0.7	BAS
99.12	30.00	0.7	BAT
97.31	30.20	0.3	BDA
99.15	25.12	-0.3	BSH
93.91	35.53	0.9	BUDO
97.50	31.00	0.2	CAD
99.26	23.13	0.0	CAY
103.76	30.91	0.1	CD2
102.92	24.68	-0.4	CHJ
98.98	18.79	0.5	CHTO
101.54	25.03	-0.7	CUX
101.90	30.88	1.0	DAB
101.32	25.73	-0.4	DAY
103.23	34.06	0.7	DBU
101.12	30.99	1.0	DFU
103.89	27.76	0.4	DGN

97.38	37.38	0.2	DLH
98.24	29.54	0.5	DNB
103.20	26.11	0.8	DUC
92.71	34.52	0.9	ERDO
99.56	26.06	-0.2	EYA
94.06	29.78	-0.3	GANZ
101.97	30.06	0.2	GDS
103.15	23.35	-0.4	GEJ
94.87	36.43	0.9	GOM
99.81	39.41	0.3	GTA
102.17	30.12	0.9	GUN
106.66	26.46	-0.1	GYA
102.58	26.64	-0.9	HDN
100.15	26.55	-0.8	HEQ
102.91	35.01	0.9	HEZ
102.75	25.15	-0.8	HLT
104.39	29.57	0.6	HMS
99.82	30.22	0.1	HNI
104.74	28.64	0.4	HWS
101.25	36.67	0.0	HYQ
99.90	26.54	-0.4	JCH
100.74	22.02	-0.2	JHO
104.54	31.01	-0.9	JJS
102.74	25.12	-1.0	KMI
100.23	26.90	0.5	LIJ
100.24	30.00	0.4	LIT
98.85	25.83	0.5	LKU
100.07	23.88	-0.1	LNC
100.75	31.30	0.9	LUH
102.45	25.54	1.0	LUQ
106.01	29.52	0.3	LZZ
103.58	25.43	-0.8	MAL
100.25	34.48	0.7	MAQI
102.22	31.89	0.9	MEK
103.39	24.41	0.7	MIL
101.56	21.48	0.2	MLA
98.60	29.70	0.8	MNK
100.52	25.05	-0.1	NAJ
106.68	35.45	0.5	PIL
101.74	26.50	-0.7	PZH
102.92	26.92	0.6	QJA
100.98	32.27	0.8	RTA
91.70	31.02	0.9	SANG
102.76	37.62	0.3	SHG
101.01	22.78	0.1	SMO
98.52	25.03	-0.2	TCG
102.75	24.07	-0.6	THI
95.20	30.06	-0.5	TMY
100.25	25.61	-0.7	TSH
97.38	29.88	-0.1	TTO
94.82	36.20	0.9	TUNL
97.48	29.42	-0.1	WDA
98.07	24.09	0.1	WDI
91.90	33.45	1.0	WNDO
104.25	23.41	-0.2	WSH
104.99	33.36	0.8	WUD
99.80	28.93	0.5	XAC
88.87	29.25	0.6	XIGA
102.77	29.34	1.0	XJP
101.02	30.03	-0.3	YAJ
105.93	38.61	-0.2	YCH
104.10	30.20	0.8	YGD

99.40	30.29	-0.2	YID
99.37	25.89	0.7	YLO
102.20	24.72	-0.5	YME
100.77	26.69	0.2	YSH
100.14	24.24	-0.5	YXI
97.02	33.01	1.0	YUS
99.70	27.82	0.6	ZHD
103.72	27.32	0.4	ZOT
101.01	24.00	-0.3	ZYA
102.39	24.18	-0.2	ESH
102.49	25.22	-0.4	FUM
100.02	31.61	0.1	GAZ
102.42	23.37	-0.6	HHE
98.61	29.26	-0.2	HLS
100.33	30.10	0.1	HOL
94.34	29.67	-0.6	LNZ
94.74	29.77	-0.5	LUL
104.30	24.88	-0.7	LUP
98.59	24.42	0.0	LUX
100.84	27.29	0.8	NLG
103.60	32.65	0.9	SOA
103.02	30.01	0.8	YAN
103.15	24.92	0.0	YIL
101.86	25.69	-0.9	YMO
103.57	30.87	0.6	YZP
104.67	31.79	0.6	ZJG
89.06	32.18	0.5	
88.86	33.02	1.0	
88.56	33.59	0.4	
101.32	25.73	-0.4	
100.07	23.88	-0.1	
98.85	25.83	0.6	
101.56	21.48	0.2	
100.52	25.05	-0.1	
98.98	18.79	0.5	
102.74	25.12	-1.0	